SIMA – Raw Data Simulation Software for the Development and Validation of Algorithms for GNSS and MEMS based Multi-Sensor Navigation Platforms

Reiner JÄGER, Julia DIEKERT, Andreas HOSCISLAWSKI and Jan ZWIENER, Germany

Key words: Low-cost GNSS, INS, raw data simulation software, multi-sensor navigation platform, lever arms, multi-sensor fusion, navigation algorithms, sensor calibration on the fly, sensor-platform design and optimization, platform-body design

SUMMARY

The development of navigation algorithms is generally dependent on the application and required specifications, on the movement characteristics of the object and on the navigation sensors to be used. To compare and analyze the performance of algorithms for the estimation of the navigation state vector they have to be provided with the same sensor data observation sets. That can be achieved through simulation of different trajectories and the calculation of resulting sensor observations. Moreover, realistic simulation of sensor array observations can boost the development and optimization of navigation platforms in respect to required accuracy and reliability.

In this paper the simulation and determination of raw sensor observations for different types of sensors is derived with appropriate sensor error models for low cost sensors, based on a predefined analytic trajectory of the object (body). Conceptually multiple platforms on a body can carry multiple sensors in a free geometric configuration that includes position as well as orientation. This leads to the so-called lever arms between sensor-platform and platform-body.

The application and validation of the presented simulation software SIMA (SImulation of Multisensor Arrays) is shown with two different mathematical models for the navigation state estimation, which are able to handle lever arms and to determine the simulated sensor errors on the fly. SIMA is capable of providing raw data observations for GNSS, accelerometers, gyroscopes, inclinometers and magnetic field sensors, and is therefore an essential tool for the development, analysis and optimization of navigation algorithms.

SIMA – Raw Data Simulation Software for the Development and Validation of Algorithms for GNSS and MEMS based Multi-Sensor Navigation Platforms

Reiner JÄGER, Julia DIEKERT, Andreas HOSCISLAWSKI and Jan ZWIENER, Germany

1. INTRODUCTION

The development of navigation algorithms essentially depends on the application, the hardware type (e.g. a smartphone) and the design of the navigation sensors on sensor platforms that are used. Collecting real data with multi-sensor platforms and the corresponding precise reference data takes a lot of time, effort and is cost-intensive. Besides the work of time synchronization, in particular for an attitude reference there is no standard procedure available in the field of low-cost. In addition there are only multi-sensor platforms with a standard, non-redundant sensor design on the market, which consists of one GNSS receiver and a three axes inertial measurement unit (IMU). Consequently raw data simulation tools are required for the development, validation and analysis of new navigation algorithms in regard of achievable accuracy, precision, reliability and robustness against sensor errors.

With the possibility to simulate any number and type of sensor, the configuration of sensors on the platform, as well as the platform-body-design can be optimized cost-effectively. These so-called lever arms (chapter 4) that result from the eccentric installation of platforms (p) on the body (b) and sensors (s) on the platform (p) can improve the estimation of the navigation state vector $\mathbf{y}(\mathrm{t}) = [(\mathrm{B}, \mathrm{L}, \mathrm{h})^{\mathrm{e}} | (\mathrm{v_N}, \mathrm{v_E}, \mathrm{v_D})^{\mathrm{n}} | (\mathrm{r}, \mathrm{p}, \mathrm{y})_{\mathrm{b}}^{\mathrm{n}}]^{\mathrm{T}}$, that is composed of the bodies position $(\mathrm{B}, \mathrm{L}, \mathrm{h})^{\mathrm{e}}$, velocity $(\mathrm{v_N}, \mathrm{v_E}, \mathrm{v_D})^{\mathrm{n}}$ and attitude $(\mathrm{r}, \mathrm{p}, \mathrm{y})_{\mathrm{b}}^{\mathrm{n}}$.

The simulation tool SIMA (SImulation of Multisensor Arrays) that is developed at University of Applied Sciences Karlsruhe, allows the generation of user-defined sensor data observations as reference data related to a given analytical model for the trajectory for a moving body and a specified sensor configuration. The observations of accelerometers, gyroscopes, magnetometers and inclinometers can be modeled under consideration of the different lever arm effects on every sensor j. Additionally, GNSS observations can be simulated, that consist of GNSS positions and velocities for loose coupled integration, or of pseudoranges, phase and Doppler measurements, that can be coupled tightly or deeply. The introduction of individual parameterized sensor error models and the possibility to create occasional gross errors results in realistic scenarios that allow the performance analysis of different navigation algorithms.

2. COORDINATE SYSTEMS AND FRAME TRANSFORMATIONS

Algorithms for multi-sensor systems require transformations of the state as well as the sensor observation equation between the inertial frame and other various global and local frames. The navigation state is usually determined in a global frame, whereas observations are tied to a local platform frame. The different frames are described in this chapter.

Inertial frame (i-frame)

Inertial sensor observations, e.g. from a accelerometer or a gyroscope, are directly related to the inertial frame (i), e.g. by $\ddot{\mathbf{x}}^{\mathrm{i}} = \mathbf{g}^{\mathrm{i}}(\mathbf{x}) + \mathbf{a}^{\mathrm{i}}$ as holds for accelerometer observations. The i-frame is considered to be free of acceleration and rotation. So a body at rest in the i-frame $\ddot{\mathbf{x}}^{\mathrm{i}} = 0$, or in the e-frame $\ddot{\mathbf{x}}^{\mathrm{e}} = 0$ respectively, would only sense the gravitational acceleration $\mathbf{g}^{\mathrm{i}}(\mathbf{x})$, in the e-frame respectively the gravitative accelerated $\ddot{\mathbf{x}}^{\mathrm{e}}$ and the centrifugal acceleration $\ddot{\mathbf{x}}^{\mathrm{e}}_{\mathrm{cent}}$. One instance of an i-frame is the International Celestial Reference Frame (ICRF), with its origin at the center of mass of the solar system. Another instance would be the Earth Centered Inertial Frame (ECIF), where the origin is located at the earth's center of mass.

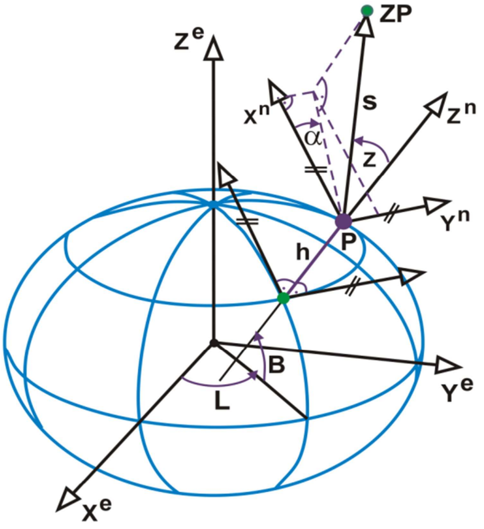

Figure 1: e-frame and n-frame

Earth-frame (e-frame)

The e-frame (fig. 1) or often called Earth Centered, Earth Fixed frame (ECEF), has the same origin as the ECIF frame but is fixed in respect to the earth. The rotation from ECIF to ECEF has to account for polar motion $\mathbf{R}_{\mathrm{P}}$, earth rotation $\mathbf{R}_{\mathrm{E}}$, nutation $\mathbf{R}_{\mathrm{N}}$ and precession $\mathbf{R}_{\mathrm{pr}}$, where $\mathbf{R}_{\mathrm{E}}$ shows the highest rotation rate ($\mathbf{\Omega}^{\mathrm{e}}_{\mathrm{ie}}$).

$$\mathbf{R}^{\mathrm{e}}_{\mathrm{i}}(\mathrm{t}) = \mathbf{R}_{\mathrm{P}} \cdot \mathbf{R}_{\mathrm{E}} \cdot \mathbf{R}_{\mathrm{N}} \cdot \mathbf{R}_{\mathrm{pr}} \qquad (2.1)$$

Geographic coordinates $(\mathrm{B}, \mathrm{L}, \mathrm{h})^{\mathrm{e}}$ can be derived from Cartesian coordinates $(\mathrm{x}, \mathrm{y}, \mathrm{z})^{\mathrm{e}}$ as:

$$\begin{bmatrix} \mathrm{x} \\ \mathrm{y} \\ \mathrm{z} \end{bmatrix}^{\mathrm{e}} = \begin{bmatrix} (\mathrm{N}(\mathrm{B}) + \mathrm{h}) \cos \mathrm{B} \cos \mathrm{L} \\ (\mathrm{N}(\mathrm{B}) + \mathrm{h}) \cos \mathrm{B} \sin \mathrm{L} \\ (\mathrm{N}(\mathrm{B})(1 - \mathrm{e}^2) + \mathrm{h}) \sin \mathrm{B} \end{bmatrix}^{\mathrm{e}} . \qquad (2.2)$$

Navigation frame (n-frame)

The n-frame is defined by the position of a navigating object. Its x and y axes are in the local tangential plane on the earth's ellipsoid and the x axis is aligned to geographical north. The down-axis is parallel to the current ellipsoidal normal. The axis of the n-frame are depicted in figure 1 with x^{n}, y^{n} and z^{n}.

Motion frame (m-frame)

This frame is similar to the position dependent n-frame, but does not follow the navigated body. Instead it is in the context with raw sensor data simulation fixed to a predefined position on earth with constant rotation matrix $\mathbf{R}^{\mathrm{e}}_{\mathrm{m}}\left(\mathrm{B}_{\mathrm{m\_origin}}, \mathrm{L}_{\mathrm{m\_origin}}\right)$. Since this frame is tangential to the earth's surface the modeling of a trajectory in the local tangential area of the m-frame is very intuitive.

Local Astronomical Vertical System (LAV)

The local astronomical vertical system can be created for an arbitrary point on the earth (like the n-frame). The z-axis of this frame is parallel to the local plumb line, and the x-axis points to geographical north. The local plumb line is spanned up by the gravity vector and differs from the ellipsoidal normal by the amount of the deflection from the vertical.

Body frame (b-frame)

The b-frame is a local frame on the body that can be freely defined. In general it is located in the center of the body and the x-axis is aligned to the main moving direction, the so-called roll axis.

Platform frame (p-frame)

The p-frame can also be arbitrarily defined, especially with respect to the position of the platform (p) on the body (b) (fig. 2). Further and in general each body can be navigated with several platforms. The orientation of the individual p-frame with respect to the b-frame is often set up in a strap-down mode.

Sensor frame (s-frame)

As a platform (p) carries several sensors (s), each sensor has its own associated sensor frame where the raw measurements are gathered. The orientation (α, δ) and the location $\mathbf{t}^{\mathrm{p}}_{\mathrm{sensor}}$ of the individual s-frame with respect to the associated p-frame are known design parameters of the sensor platform.

3. MODELING OF THE NAVIGATION STATE WITH A GIVEN TRAJECTORY

In the SIMA concept the state vector $\mathbf{y}(\mathrm{t})$ is modeled by a given trajectory and prescribed body orientation along the track, and the sensor observations result uniquely from that state $\mathbf{y}(\mathrm{t})$. So the navigation state $\mathbf{y}(\mathrm{t})$ and the respective sensor observation state $\mathbf{l}(\mathrm{t})$ can be regarded as reference states $[\mathbf{y}(\mathrm{t}), \mathbf{l}(\mathrm{t})]_{\mathrm{ref}}$. Based on the given trajectory the position $\mathbf{x}(\mathrm{t})$, velocity $\dot{\mathbf{x}}(\mathrm{t})$, acceleration $\ddot{\mathbf{x}}(\mathrm{t})$, orientation $\mathbf{R}(\mathrm{t})$, rotation rate $\boldsymbol{\Omega}(\mathrm{t})$ and the change of the rotation rate $\dot{\boldsymbol{\Omega}}(\mathrm{t})$ of the body (b) dependent on the time t can be derived. One method is to use a Cartesian coordinate system, in which the motion is modeled, for example the m-frame.

$$\mathbf{x}(\mathrm{t})^{\mathrm{m}}_{\mathrm{body}} = \begin{bmatrix} \mathrm{r}_{circ}\cos(\mathrm{v\,t} / \mathrm{r}_{circ}) \\ \mathrm{r}_{circ}\sin(\mathrm{v\,t} / \mathrm{r}_{circ}) \\ 0.0 \end{bmatrix} \qquad \mathrm{r}^{\mathrm{m}}_{\mathrm{b}} = \mathrm{p}^{\mathrm{m}}_{\mathrm{b}} = 0$$

$$\mathrm{y(t)}^{\mathrm{m}}_{\mathrm{b}} = \mathrm{atan}\left(\frac{\cos(\mathrm{v\,t} / \mathrm{r}_{circ})}{-\sin(\mathrm{v\,t} / \mathrm{r}_{circ})}\right)$$

$$\dot{\mathbf{x}}(t)^{\mathrm{m}}_{\mathrm{body}} = \begin{bmatrix} -\mathrm{v}\sin(\mathrm{v\,t} / \mathrm{r}_{circ}) \\ \mathrm{v}\cos(\mathrm{v\,t} / \mathrm{r}_{circ}) \\ 0.0 \end{bmatrix} \qquad \boldsymbol{\Omega}^{\mathrm{b}}_{\mathrm{mb}} = \begin{bmatrix} 0 & -\mathrm{v}/\mathrm{r}_{circ} & 0 \\ \mathrm{v}/\mathrm{r}_{circ} & 0 & 0 \\ 0 & 0 & 0 \end{bmatrix} \tag{3.1}$$

$$\ddot{\mathbf{x}}(t)^{\mathrm{m}}_{\mathrm{body}} = \begin{bmatrix} -\mathrm{v}^2 / \mathrm{r}_{circ}\cos(\mathrm{v\,t} / \mathrm{r}_{circ}) \\ -\mathrm{v}^2 / \mathrm{r}_{circ}\sin(\mathrm{v\,t} / \mathrm{r}_{circ}) \\ 0.0 \end{bmatrix} \qquad \dot{\boldsymbol{\Omega}}^{\mathrm{b}}_{\mathrm{mb}} = \begin{bmatrix} 0 & 0 & 0 \\ 0 & 0 & 0 \\ 0 & 0 & 0 \end{bmatrix}$$

A simple but interesting analytic curve is a circle. If its radius r_{circ} and the velocity v of the body (b) in the direction of the x-axis (roll axis) are defined on the circle, the time dependent position $\mathbf{x}(\mathrm{t})^{\mathrm{m}}_{\mathrm{body}}$, velocity $\dot{\mathbf{x}}(\mathrm{t})^{\mathrm{m}}_{\mathrm{body}}$, acceleration $\ddot{\mathbf{x}}(\mathrm{t})^{\mathrm{m}}_{\mathrm{body}}$, orientation $\mathbf{R}(\mathrm{t})^{\mathrm{m}}_{\mathrm{b}}$, which is defined by the angles $\mathrm{r}^{\mathrm{m}}_{\mathrm{b}}$, $\mathrm{p}^{\mathrm{m}}_{\mathrm{b}}$ and $\mathrm{y}^{\mathrm{m}}_{\mathrm{b}}$, the rotation rate $\mathbf{\Omega}^{\mathrm{b}}_{\mathrm{mb}}$ and the change of the rotation rate $\dot{\mathbf{\Omega}}^{\mathrm{b}}_{\mathrm{mb}}$ of the body (b) in the m-frame can be calculated from the system of equations (3.1).
In this example it is always assumed, that the yaw angle $\mathrm{y}^{\mathrm{m}}_{\mathrm{b}}$ of the body regarding the m-frame is aligned to the trajectory's tangent and roll $\mathrm{r}^{\mathrm{m}}_{\mathrm{b}}$ and pitch $\mathrm{p}^{\mathrm{m}}_{\mathrm{b}}$ are zero in the plane of the circle. In a general case the orientation of the body is independent from the trajectory.
In most simulation equations the position, velocity and acceleration of the body (b) is required in the global e-frame. This transformation is done in SIMA in a second step based on (3.2), where $\mathbf{x}^{\mathrm{e}}_{\mathrm{m\_origin}}$ is the origin of the m-frame in Cartesian coordinates of the e-frame:

$$\begin{aligned}\mathbf{x}(\mathrm{t})^{\mathrm{e}}_{\mathrm{body}} &= \mathbf{x}^{\mathrm{e}}_{\mathrm{m\_origin}} + \mathbf{R}^{\mathrm{e}}_{\mathrm{m}}\mathbf{x}^{\mathrm{m}}_{\mathrm{body}}\\ \dot{\mathbf{x}}(\mathrm{t})^{\mathrm{e}}_{\mathrm{body}} &= \mathbf{R}^{\mathrm{e}}_{\mathrm{m}}\dot{\mathbf{x}}^{\mathrm{m}}_{\mathrm{body}}\\ \ddot{\mathbf{x}}(\mathrm{t})^{\mathrm{e}}_{\mathrm{body}} &= \mathbf{R}^{\mathrm{e}}_{\mathrm{m}}\ddot{\mathbf{x}}^{\mathrm{m}}_{\mathrm{body}}.\end{aligned} \tag{3.2}$$

4. LEVER ARM CONCEPT

For the determination of the complete navigation state $\mathbf{y}(\mathrm{t})$ of the body (b) multiple sensors j (j=1,n) and different types of sensors have to be integrated to estimate an optimal navigation solution $\mathbf{y}(\mathrm{t})$. Since the amount of space and volume on a platform is limited and all sensors cannot be installed at the center of the body (b) by practical reasons, the sensor distance from sensor to platform center, and the distance between platform and b-frame, that are combined in the so-called lever arm, have to be considered in the navigation algorithms and in the simulation of the observations (SIMA-software).
Therefore the sensor position $\mathbf{t}^{\mathrm{p}}_{\mathrm{sensor}}$ and orientation $\mathbf{R}(\alpha,\delta)^{\mathrm{p}}_{\mathrm{s}}$ of the j-th sensor on the i-th platform $\left[\mathbf{t}^{\mathrm{p}}_{\mathrm{sensor}}, \mathbf{R}(\alpha,\delta)^{\mathrm{p}}_{\mathrm{s}}\right]_{\mathrm{i,j}}$ is parametrized in the p-frame (fig. 2) with α and δ as angles between sensitive sensor axis x^s and xy-plane respectively xz-plane of the platform frame (p). The transformation between platform and body is defined with six additional parameters: Position $\mathbf{t}^{\mathrm{b}}_{\mathrm{plat}}\left(x^b_{plat}, y^b_{plat}, z^b_{plat}\right)$ and orientation $\mathbf{R}^{\mathrm{b}}_{\mathrm{p}}(\varepsilon_x, \varepsilon_y, \varepsilon_z)$ of the i-th platform (p) on the body.
The position of the sensor $\mathbf{x}(\mathrm{t})^{\mathrm{e}}_{\mathrm{sensor}}$ (fig 2) in the e-frame is presented under consideration of the lever arms, which consists of $\mathbf{t}^{\mathrm{e}}_{\mathrm{plat}}$ and $\mathbf{t}(\mathrm{t})^{\mathrm{e}}_{\mathrm{sensor}}$ and reads:

$$\Big[\mathbf{x}(\mathrm{t})^{\mathrm{e}}_{\mathrm{sensor}} = \mathbf{x}(\mathrm{t})^{\mathrm{e}}_{\mathrm{body}} + \mathbf{t}^{\mathrm{e}}_{\mathrm{plat}} + \mathbf{t}(\mathrm{t})^{\mathrm{e}}_{\mathrm{sensor}} = \mathbf{x}(\mathrm{t})^{\mathrm{e}}_{\mathrm{body}} + \mathbf{R}^{\mathrm{e}}_{\mathrm{m}}\mathbf{R}(\mathrm{t})^{\mathrm{m}}_{\mathrm{b}}\mathbf{R}^{\mathrm{b}}_{\mathrm{p}}\mathbf{t}^{\mathrm{p}}_{\mathrm{plat}} + \mathbf{R}^{\mathrm{e}}_{\mathrm{m}}\mathbf{R}(\mathrm{t})^{\mathrm{m}}_{\mathrm{b}}\mathbf{R}^{\mathrm{b}}_{\mathrm{p}}\mathbf{R}(\mathrm{t})^{\mathrm{p}}_{\mathrm{s}}\mathbf{t}^{\mathrm{s}}_{\mathrm{sensor}}\Big]_{\mathrm{i,j}}. \tag{4.1}$$

To derive the velocity (eq. 4.2) and acceleration (eq. 4.3) that drive the observations of a sensor j on platform i, (eq. 4.1) has to be differentiated in respect to time t, taking into account that position and orientation of the platform i regarding the body (b) are constant. For a sensor j it is assumed instead, that its position and orientation on the platform i are able to change with time. A reason to create time-dynamic sensor-platform-parameters can be to calibrate

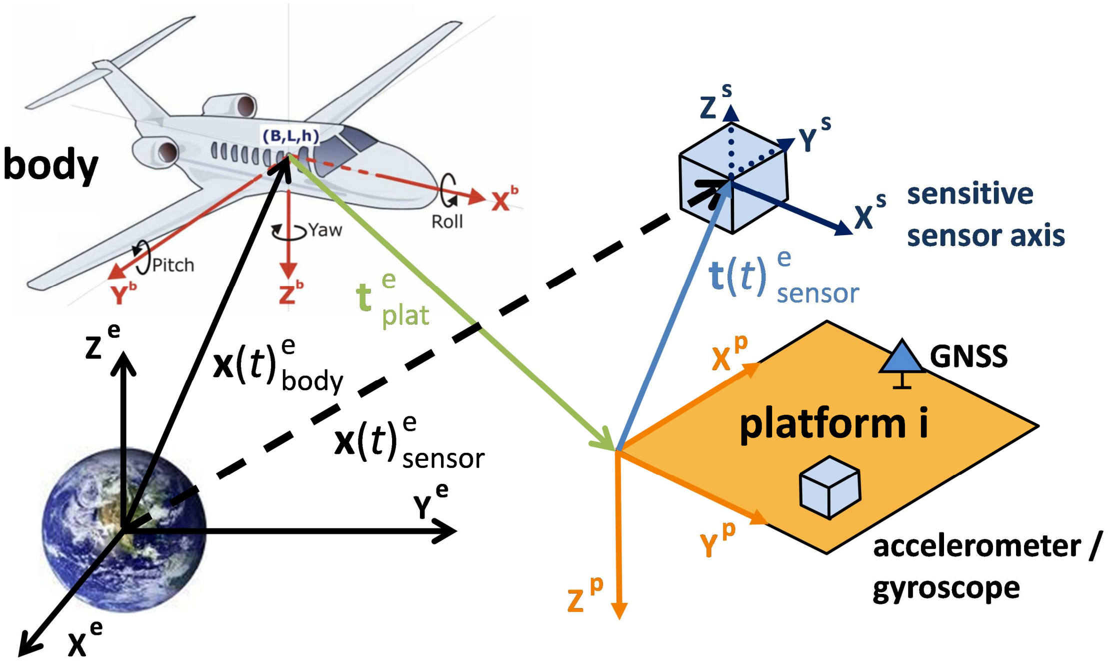

Figure 2: Geometry and lever arm parametrization in a multi-platform-multi-sensor navigation design

specific sensor errors, for example, if the sensitive axes have to be coupled to the gravity vector (Wendel, 2007). Because the sensor calibration on the fly depends on the body trajectory, some sensors can only be calibrated poorly. With a rotation of the sensor axis on the platform the calibration procedure can be optimized. For the velocity and acceleration of the sensor we get from (4.1):

$$\left[\begin{aligned}\frac{\partial}{\partial \mathrm{t}}\mathbf{x}(\mathrm{t})^{\mathrm{e}}_{\mathrm{sensor}} &= \dot{\mathbf{x}}(\mathrm{t})^{\mathrm{e}}_{\mathrm{sensor}}\\ &= \dot{\mathbf{x}}(\mathrm{t})^{\mathrm{e}}_{\mathrm{body}} + \mathbf{R}^{\mathrm{e}}_{\mathrm{m}}\mathbf{R}^{\mathrm{m}}_{\mathrm{b}}\boldsymbol{\Omega}^{\mathrm{b}}_{\mathrm{mb}}\mathbf{R}^{\mathrm{b}}_{\mathrm{p}}\mathbf{t}^{\mathrm{p}}_{\mathrm{plat}} + \mathbf{R}^{\mathrm{e}}_{\mathrm{m}}\mathbf{R}^{\mathrm{m}}_{\mathrm{b}}\boldsymbol{\Omega}^{\mathrm{b}}_{\mathrm{mb}}\mathbf{R}^{\mathrm{b}}_{\mathrm{p}}\mathbf{R}^{\mathrm{p}}_{\mathrm{s}}\mathbf{t}^{\mathrm{s}}_{\mathrm{sensor}}\\ &\quad + \mathbf{R}^{\mathrm{e}}_{\mathrm{m}}\mathbf{R}^{\mathrm{m}}_{\mathrm{b}}\mathbf{R}^{\mathrm{b}}_{\mathrm{p}}\mathbf{R}^{\mathrm{p}}_{\mathrm{s}}\boldsymbol{\Omega}^{\mathrm{s}}_{\mathrm{ps}}\mathbf{t}^{\mathrm{s}}_{\mathrm{sensor}} + \mathbf{R}^{\mathrm{e}}_{\mathrm{m}}\mathbf{R}^{\mathrm{m}}_{\mathrm{b}}\mathbf{R}^{\mathrm{b}}_{\mathrm{p}}\mathbf{R}^{\mathrm{p}}_{\mathrm{s}}\dot{\mathbf{t}}^{\mathrm{s}}_{\mathrm{sensor}}\end{aligned}\right]_{\mathrm{i,j}} \tag{4.2}$$

and

$$\left[\begin{aligned}\frac{\partial}{\partial \mathrm{t}}\dot{\mathbf{x}}(\mathrm{t})^{\mathrm{e}}_{\mathrm{sensor}} &= \ddot{\mathbf{x}}(\mathrm{t})^{\mathrm{e}}_{\mathrm{sensor}}\\ &= \ddot{\mathbf{x}}^{\mathrm{e}}_{\mathrm{body}} + \mathbf{R}^{\mathrm{e}}_{\mathrm{m}}\mathbf{R}^{\mathrm{m}}_{\mathrm{b}}\boldsymbol{\Omega}^{\mathrm{b}}_{\mathrm{mb}}\boldsymbol{\Omega}^{\mathrm{b}}_{\mathrm{mb}}\mathbf{R}^{\mathrm{b}}_{\mathrm{p}}\mathbf{t}^{\mathrm{p}}_{\mathrm{plat}} + \mathbf{R}^{\mathrm{e}}_{\mathrm{m}}\mathbf{R}^{\mathrm{m}}_{\mathrm{b}}\dot{\boldsymbol{\Omega}}^{\mathrm{b}}_{\mathrm{mb}}\mathbf{R}^{\mathrm{b}}_{\mathrm{p}}\mathbf{t}^{\mathrm{p}}_{\mathrm{plat}}\\ &\quad + \mathbf{R}^{\mathrm{e}}_{\mathrm{m}}\mathbf{R}^{\mathrm{m}}_{\mathrm{b}}\boldsymbol{\Omega}^{\mathrm{b}}_{\mathrm{mb}}\boldsymbol{\Omega}^{\mathrm{b}}_{\mathrm{mb}}\mathbf{R}^{\mathrm{b}}_{\mathrm{p}}\mathbf{R}^{\mathrm{p}}_{\mathrm{s}}\mathbf{t}^{\mathrm{s}}_{\mathrm{sensor}} + \mathbf{R}^{\mathrm{e}}_{\mathrm{m}}\mathbf{R}^{\mathrm{m}}_{\mathrm{b}}\dot{\boldsymbol{\Omega}}^{\mathrm{b}}_{\mathrm{mb}}\mathbf{R}^{\mathrm{b}}_{\mathrm{p}}\mathbf{R}^{\mathrm{p}}_{\mathrm{s}}\mathbf{t}^{\mathrm{s}}_{\mathrm{sensor}}\\ &\quad + \mathbf{R}^{\mathrm{e}}_{\mathrm{m}}\mathbf{R}^{\mathrm{m}}_{\mathrm{b}}\boldsymbol{\Omega}^{\mathrm{b}}_{\mathrm{mb}}\mathbf{R}^{\mathrm{b}}_{\mathrm{p}}\mathbf{R}^{\mathrm{p}}_{\mathrm{s}}\boldsymbol{\Omega}^{\mathrm{s}}_{\mathrm{ps}}\mathbf{t}^{\mathrm{s}}_{\mathrm{sensor}} + \mathbf{R}^{\mathrm{e}}_{\mathrm{m}}\mathbf{R}^{\mathrm{m}}_{\mathrm{b}}\boldsymbol{\Omega}^{\mathrm{b}}_{\mathrm{mb}}\mathbf{R}^{\mathrm{b}}_{\mathrm{p}}\mathbf{R}^{\mathrm{p}}_{\mathrm{s}}\dot{\mathbf{t}}^{\mathrm{s}}_{\mathrm{sensor}}\\ &\quad + \mathbf{R}^{\mathrm{e}}_{\mathrm{m}}\mathbf{R}^{\mathrm{m}}_{\mathrm{b}}\boldsymbol{\Omega}^{\mathrm{b}}_{\mathrm{mb}}\mathbf{R}^{\mathrm{b}}_{\mathrm{p}}\mathbf{R}^{\mathrm{p}}_{\mathrm{s}}\boldsymbol{\Omega}^{\mathrm{s}}_{\mathrm{ps}}\mathbf{t}^{\mathrm{s}}_{\mathrm{sensor}} + \mathbf{R}^{\mathrm{e}}_{\mathrm{m}}\mathbf{R}^{\mathrm{m}}_{\mathrm{b}}\mathbf{R}^{\mathrm{b}}_{\mathrm{p}}\mathbf{R}^{\mathrm{p}}_{\mathrm{s}}\boldsymbol{\Omega}^{\mathrm{s}}_{\mathrm{ps}}\boldsymbol{\Omega}^{\mathrm{s}}_{\mathrm{ps}}\mathrm{t}^{\mathrm{s}}_{\mathrm{sensor}}\\ &\quad + \mathbf{R}^{\mathrm{e}}_{\mathrm{m}}\mathbf{R}^{\mathrm{m}}_{\mathrm{b}}\mathbf{R}^{\mathrm{b}}_{\mathrm{p}}\mathbf{R}^{\mathrm{p}}_{\mathrm{s}}\dot{\boldsymbol{\Omega}}^{\mathrm{s}}_{\mathrm{ps}}\mathbf{t}^{\mathrm{s}}_{\mathrm{sensor}} + \mathbf{R}^{\mathrm{e}}_{\mathrm{m}}\mathbf{R}^{\mathrm{m}}_{\mathrm{b}}\mathbf{R}^{\mathrm{b}}_{\mathrm{p}}\mathbf{R}^{\mathrm{p}}_{\mathrm{s}}\boldsymbol{\Omega}^{\mathrm{s}}_{\mathrm{ps}}\dot{\mathbf{t}}^{\mathrm{s}}_{\mathrm{sensor}}\\ &\quad + \mathbf{R}^{\mathrm{e}}_{\mathrm{m}}\mathbf{R}^{\mathrm{m}}_{\mathrm{b}}\boldsymbol{\Omega}^{\mathrm{b}}_{\mathrm{mb}}\mathbf{R}^{\mathrm{b}}_{\mathrm{p}}\mathbf{R}^{\mathrm{p}}_{\mathrm{s}}\dot{\mathbf{t}}^{\mathrm{s}}_{\mathrm{sensor}} + \mathbf{R}^{\mathrm{e}}_{\mathrm{m}}\mathbf{R}^{\mathrm{m}}_{\mathrm{b}}\mathbf{R}^{\mathrm{b}}_{\mathrm{p}}\mathbf{R}^{\mathrm{p}}_{\mathrm{s}}\boldsymbol{\Omega}^{\mathrm{s}}_{\mathrm{ps}}\dot{\mathbf{t}}^{\mathrm{s}}_{\mathrm{sensor}}\\ &\quad + \mathbf{R}^{\mathrm{e}}_{\mathrm{m}}\mathbf{R}^{\mathrm{m}}_{\mathrm{b}}\mathbf{R}^{\mathrm{b}}_{\mathrm{p}}\mathbf{R}^{\mathrm{p}}_{\mathrm{s}}\ddot{\mathbf{t}}^{\mathrm{s}}_{\mathrm{sensor}}\end{aligned}\right]_{i,j}. \tag{4.3}$$

5. GNSS OBSERVATIONS

In general the GNSS component is part of a multi sensor array and so of fusion algorithms on various integration levels. On the level of loose coupled integration schemes only the calculated position and velocity solution of a GNSS receiver is considered (chap. 5.1). On the level of tight or deep coupling the GNSS raw data (pseudorange, phase measurement and Doppler frequency) are integrated as observations into the navigation algorithms.

5.1 GNSS position and velocity modeling

The position and velocity solution of a real GNSS receiver is commonly provided in the e-frame. Since the position $\mathbf{x}(\mathrm{t})^{\mathrm{e}}_{\mathrm{body}}$ and velocity $\dot{\mathbf{x}}(\mathrm{t})^{\mathrm{e}}_{\mathrm{body}}$ of a simulated object is known as a time-dependent function of the object's trajectory according to chapter 3, the simulation of such a position and velocity as observation output of SIMA for the GNSS receiver j in the e-frame, only the individual lever arm of the GNSS sensor j has to be considered.
For the modeling of the GNSS position $\mathbf{x}^{\mathrm{e}}_{\mathrm{GNSS-pos}}$ we start from equation (4.1). The position of a platform i is defined in the b-frame, the position of the sensor j in the p-frame. Assuming the position and orientation of a GNSS receiver are constant regarding the platform equation (5.1) can be obtained.

$$\begin{aligned}\Big[\mathbf{x}^{\mathrm{e}}_{\mathrm{GNSS-pos}} &= \mathbf{x}(\mathrm{t})^{\mathrm{e}}_{\mathrm{body}} + \mathbf{R}^{\mathrm{e}}_{\mathrm{m}}\mathbf{R}(\mathrm{t})^{\mathrm{m}}_{\mathrm{b}}\mathbf{t}^{\mathrm{b}}_{\mathrm{plat}} + \mathbf{R}^{\mathrm{e}}_{\mathrm{m}}\mathbf{R}(\mathrm{t})^{\mathrm{m}}_{\mathrm{b}}\mathbf{R}^{\mathrm{b}}_{\mathrm{p}}\mathbf{t}^{\mathrm{p}}_{\mathrm{sensor}} \\ &= \mathbf{x}(\mathrm{t})^{\mathrm{e}}_{\mathrm{body}} + \mathbf{LA}(\mathrm{t})^{\mathrm{e}}_{\mathrm{pos}}\Big]_{\mathrm{i,j}}\end{aligned} \tag{5.1}$$

Individual sensor noise $\mathbf{n}^{\mathrm{e}}_{\mathrm{GNSS-pos}}$ can be added to sensor j in equation (5.1) and with equation (5.2) the final equation to simulate the GNSS position observation $\left[\mathbf{l}^{\mathrm{e}}_{\mathrm{GNSS-pos}}\right]_{\mathrm{i,j}}$ is given.

$$\left[\mathbf{l}^{\mathrm{e}}_{\mathrm{GNSS-pos}}\right]_{\mathrm{i,j}} = \left[\mathbf{x}^{\mathrm{e}}_{\mathrm{GNSS-pos}} + \mathbf{n}^{\mathrm{e}}_{\mathrm{GNSS-pos}}\right]_{\mathrm{i,j}} \tag{5.2}$$

Similar to the GNSS position the GNSS velocity observation is simulated (eq. 5.3), starting with equation (4.2) and with the same assumptions as in the GNSS position simulation.

$$\begin{aligned}\Big[\dot{\mathbf{x}}^{\mathrm{e}}_{\mathrm{GNSS-vel}} &= \dot{\mathbf{x}}(\mathrm{t})^{\mathrm{e}}_{\mathrm{body}} + \mathbf{R}^{\mathrm{e}}_{\mathrm{m}}\mathbf{R}^{\mathrm{m}}_{\mathrm{b}}\mathbf{\Omega}^{\mathrm{b}}_{\mathrm{mb}}\mathbf{t}^{\mathrm{b}}_{\mathrm{plat}} + \mathbf{R}^{\mathrm{e}}_{\mathrm{m}}\mathbf{R}^{\mathrm{m}}_{\mathrm{b}}\mathbf{\Omega}^{\mathrm{b}}_{\mathrm{mb}}\mathbf{R}^{\mathrm{b}}_{\mathrm{p}}\mathbf{t}^{\mathrm{p}}_{\mathrm{sensor}} \\ &= \dot{\mathbf{x}}(\mathrm{t})^{\mathrm{e}}_{\mathrm{body}} + \mathbf{LA}(\mathrm{t})^{\mathrm{e}}_{\mathrm{vel}}\Big]_{\mathrm{i,j}}\end{aligned} \tag{5.3}$$

Individual sensor noise $\mathbf{n}^{\mathrm{e}}_{\mathrm{GNSS-vel}}$ can be added, too, so the final GNSS velocity observation $[\mathbf{l}^{\mathrm{e}}_{\mathrm{GNSS-vel}}]_{\mathrm{i,j}}$ is given in equation (5.4).

$$[\mathbf{l}^{\mathrm{e}}_{\mathrm{GNSS-vel}}]_{\mathrm{i,j}} = [\dot{\mathbf{x}}^{\mathrm{e}}_{\mathrm{GNSS-vel}} + \mathbf{n}^{\mathrm{e}}_{\mathrm{GNSS-vel}}]_{\mathrm{i,j}} \tag{5.4}$$

5.2 GNSS raw data modeling

In a tight or deep integration scheme the GNSS raw data has to be integrated and thus simulated in SIMA. For simulation of pseudoranges, phase measurements and Doppler frequency shifts not only the trajectory of the body has to be known, but also the state of all satellites, that shall be included into the simulation. The satellite ephemerides can be calculated directly from Keplerian elements (Kaplan & Hegarty, 2006) or from real precise ephemerides, that are provided with interpolation points every 15 minutes, for example from the IGS (International GNSS Service), to get very realistic satellite constellations. These interpolation points can be used to determine the satellite position at any given time t. Using Lagrange interpolation (5.5) the coordinates $(\mathrm{x},\mathrm{y},\mathrm{z})(t)^{\mathrm{e}}_{\mathrm{sat,k}}$ of satellite k in the e-frame are interpolated as scalar values $f(t)$ with m interpolation points.

$$f(t) = \sum_{j=0}^{m} L_j(t)\; f(t_j) \qquad \text{with } L_j(t) = \prod_{\substack{k=0\\k\neq j}}^{m} \frac{t-t_k}{t_j-t_k} \tag{5.5}$$

It can be shown, that a 9th order interpolation polynomial is sufficient for centimeter level while 17th order interpolation is used for a millimeter level interpolation (Hofmann-Wellenhof et al., 1992).

5.3 Simulation of pseudoranges, phase measurements and Doppler frequency

Based on the known position of any satellite $\mathbf{x}^{\mathrm{e}}_{\mathrm{sat,k}}$ from chapter (5.2) and the position of the GNSS receiver $\mathbf{x}^{\mathrm{e}}_{\mathrm{GNSS-pos,j}}$ from equation (5.1), the pseudorange observation $\left[l_{PR,k}\right]_{i,j}$ from satellite k to the GNSS receiver j can be calculated directly with known speed of light c as:

$$\left[l_{PR,k}\right]_{i,j} = \left[\left|\mathbf{x}^{\mathrm{e}}_{\mathrm{GNSS-pos,j}} - \mathbf{x}^{\mathrm{e}}_{\mathrm{sat,k}}\right| + \mathrm{c}\left(\Delta\mathrm{t}_{\mathrm{GNSS,j}} - \Delta\mathrm{t}_{\mathrm{sat,k}}\right)\right]_{i,j} + \Delta\mathrm{Ion} + \Delta\mathrm{Trop} + n_{PR} \tag{5.6}$$

In the SIMA-simulation the difference between satellite and receiver clock can be introduced as fix value or with clock errors to get a more realistic simulation. Additional errors coming from ionosphere and troposphere and other signal propagation influencing effects can be integrated also, but usually only standard models for ionosphere and troposphere are included into the simulation to get a general estimation of these effects.

The phase measurements $\left[\mathrm{l}_{\phi,\mathrm{k,Li}}\right]_{\mathrm{i,j}}$can be simulated analogue directly from the known receiver and satellite positions for both GNSS frequencies (5.7).

$$\begin{aligned}\left[\mathrm{l}_{\phi,\mathrm{k,Li}}\right]_{\mathrm{i,j}} = \Big[\left|\mathbf{x}^{\mathrm{e}}_{\mathrm{GNSS-pos,j}} - \mathbf{x}^{\mathrm{e}}_{\mathrm{sat,k}}\right| + \mathrm{c}\left(\Delta\mathrm{t}_{\mathrm{GNSS,j}} - \Delta\mathrm{t}_{\mathrm{sat,k}}\right) - \left(\lambda_{\mathrm{Li}}\mathrm{N}^{\mathrm{k}}_{\mathrm{Li}}\right)_{t0} \\ - \left(\lambda_{\mathrm{Li}}\mathrm{D}^{\mathrm{k}}_{\mathrm{Li}}\right)_{ti}\Big]_{\mathrm{i,j}} - \Delta\mathrm{Ion} + \Delta\mathrm{Trop} + n_{\phi} \\ \text{with } \lambda_{\mathrm{Li}}\text{= wave length of GNSS carrier signal} \\ \text{and } \mathrm{N}^{\mathrm{k}}_{\mathrm{Li,t0}} = \mathrm{int}\left[\frac{\left|\mathbf{x}^{\mathrm{e}}_{\mathrm{GNSS-pos,j}} - \mathbf{x}^{\mathrm{e}}_{\mathrm{sat,k}}\right|}{\lambda_{\mathrm{Li}}}\right]_{t0},\ \mathrm{D}^{\mathrm{k}}_{\mathrm{Li,ti}} = \mathrm{int}\left[\int_{\mathrm{t0}}^{ti}(f_{rec} - f_{sat})\Delta\mathrm{t}\right]\end{aligned} \tag{5.7}$$

The Doppler frequency of a received signal depends on satellite and receiver position and additionally on the satellite velocities $\dot{\mathbf{x}}^{\mathrm{e}}_{\mathrm{sat,k}}$ and the velocity of the receiver $\dot{\mathbf{x}}^{\mathrm{e}}_{\mathrm{GNSS-vel}}$ that are known from the ephemerides simulation and the modeled body trajectory. This results in equation (5.8) for the simulation of the Doppler frequency shift observation $[\mathrm{l}_{\Delta\mathrm{f}}]_{i,j}$.

$$[\mathrm{l}_{\Delta\mathrm{f}}]_{i,j} = \left[\mathrm{f}_{\mathrm{sat}}\left(1 + \frac{\left(\dot{\mathbf{x}}^{\mathrm{e}}_{\mathrm{sat,k}} - \dot{\mathbf{x}}^{\mathrm{e}}_{\mathrm{GNSS-vel}}\right)\mathbf{r}^{\mathrm{e}}}{\mathrm{c}}\right) - \mathrm{f}_{\mathrm{sat}}\right]_{i,j} + n_{\Delta\mathrm{f}} \tag{5.8}$$

with $\mathrm{f}_{\mathrm{sat}}$= frequency of satellite and $\mathbf{r}^{\mathrm{e}} = \mathrm{norm}\left(\mathbf{x}^{\mathrm{e}}_{\mathrm{GNSS-pos,j}} - \mathbf{x}^{\mathrm{e}}_{\mathrm{sat,k}}\right)$

6. ACCELEROMETER OBSERVATIONS

In chapter 4 the basics for position, velocity and acceleration (4.1, 4.2, 4.3), the so-called driving forces, of sensor observations in the e-frame are derived as a function of the body trajectory and the sensor's individual lever arm. In addition to these driving forces $\frac{\partial}{\partial \mathrm{t}}\dot{\mathbf{x}}^{\mathrm{e}}_{\mathrm{acc}} = \ddot{\mathbf{x}}^{\mathrm{e}}_{\mathrm{acc}}$, that are generated by the body movement and depend on the lever arm, further accelerations occur on relating the navigation equations from the i-frame to the e-frame (Jekeli, 2001). These accelerations are the gravity $\mathbf{g}^{\mathrm{e}}_{\mathrm{acc}}$ of the earth, the centrifugal acceleration $\mathbf{\Omega}^{\mathrm{e}}_{\mathrm{ie}}\mathbf{\Omega}^{\mathrm{e}}_{\mathrm{ie}}\mathbf{x}^{\mathrm{e}}_{\mathrm{acc}}$ and the Coriolis force $2\mathbf{\Omega}^{\mathrm{e}}_{\mathrm{ie}}\dot{\mathbf{x}}^{\mathrm{e}}_{\mathrm{acc}}$, which depends on sensor position and velocity. We have:

$$\mathbf{a}^{\mathrm{e}}_{\mathrm{acc}} = \frac{\partial}{\partial \mathrm{t}}\dot{\mathbf{x}}^{\mathrm{e}}_{\mathrm{acc}} - \mathbf{g}(\mathbf{x}^{\mathrm{e}}_{\mathrm{acc}})^{\mathrm{e}}_{\mathrm{acc}} + 2\mathbf{\Omega}^{\mathrm{e}}_{\mathrm{ie}}\dot{\mathbf{x}}^{\mathrm{e}}_{\mathrm{acc}} + \mathbf{\Omega}^{\mathrm{e}}_{\mathrm{ie}}\mathbf{\Omega}^{\mathrm{e}}_{\mathrm{ie}}\mathbf{x}^{\mathrm{e}}_{\mathrm{acc}}. \tag{6.1}$$

The position $\mathbf{x}^{\mathrm{e}}_{\mathrm{acc}}$ of the j-th accelerometer on the i-th platform in equation (6.1) can be obtained from equation (4.1), as well as the velocity $\dot{\mathbf{x}}^{\mathrm{e}}_{\mathrm{acc}}$ from equation (4.2) and the "driving force" accelerations $\frac{\partial}{\partial \mathrm{t}}\dot{\mathbf{x}}^{\mathrm{e}}_{\mathrm{acc}}$ from equation (4.3). The gravitation $\mathbf{g}(\mathbf{x}^{\mathrm{e}}_{\mathrm{acc}})^{\mathrm{e}}_{\mathrm{acc}}$ depends on the position of the accelerometer and can be modeled by deriving the gravitational potential V_{E} in using a gravitational model like the EIGEN-5C, which is provided by the International Centre for Global Earth Models (ICGEM) or the GRS80 reference ellipsoid.

The accelerometer observation for a sensor j on platform i is a scalar observation in the sensitive x-axis of the s-frame (fig. 2), so the acceleration vector in the e-frame from (6.1) has to be rotated to the s-frame with (6.2) and multiplied from the left with $(1 \quad 0 \quad 0)$ (6.3).

$$\mathbf{a}^{\mathrm{s}}_{\mathrm{acc}} = \mathbf{R}^{\mathrm{s}}_{\mathrm{p}}\mathbf{R}^{\mathrm{p}}_{\mathrm{b}}\mathbf{R}^{\mathrm{b}}_{\mathrm{m}}\mathbf{R}^{\mathrm{m}}_{\mathrm{e}}\mathbf{a}^{\mathrm{e}}_{\mathrm{acc}} \tag{6.2}$$

$$[\mathrm{a}^{\mathrm{s}}_{\mathrm{acc}}]_{\mathrm{i,j}} = (1 \quad 0 \quad 0) \cdot \mathbf{a}^{\mathrm{s}}_{\mathrm{acc}} \tag{6.3}$$

In the s-frame additional sensor errors can be added to the true observation $[\mathrm{a}^{\mathrm{s}}_{\mathrm{acc}}]_{\mathrm{i,j}}$ to get the simulated observation $[\mathrm{l}^{\mathrm{s}}_{\mathrm{acc}}]_{\mathrm{i,j}}$. The standard parametrization of the error model consists of the parameters bias $\mathrm{b}^{\mathrm{s}}_{\mathrm{acc}}$, the scale factor $\kappa^{\mathrm{s}}_{\mathrm{acc}}$ and additional white noise $\mathrm{n}^{\mathrm{s}}_{\mathrm{acc}}$ and reads:

$$[\mathrm{l}^{\mathrm{s}}_{\mathrm{acc}}]_{\mathrm{i,j}} = [\mathrm{a}^{\mathrm{s}}_{\mathrm{acc}}]_{\mathrm{i,j}} \cdot \kappa^{\mathrm{s}}_{\mathrm{acc}} + \mathrm{b}^{\mathrm{s}}_{\mathrm{acc}} + \mathrm{n}^{\mathrm{s}}_{\mathrm{acc}}. \tag{6.4}$$

7. GYROSCOPE OBSERVATIONS

A gyroscope triad $\boldsymbol{\omega}^{\mathrm{s}}_{\mathrm{is}}$ measures its angular velocity with respect to the i-frame in coordinates of the s-frame. This means that all rotation rates of the single frames contribute to the observation and reads:

$$\boldsymbol{\omega}_{is}^{s} = \boldsymbol{\omega}_{ie}^{s} + \boldsymbol{\omega}_{em}^{s} + \boldsymbol{\omega}_{mb}^{s} + \boldsymbol{\omega}_{bp}^{s} + \boldsymbol{\omega}_{ps}^{s}. \tag{7.1}$$

With the assumptions that the rotation rate of the m-frame regarding the e-frame and the rotation rate of the p-frame regarding the b-frame are zero we get equation (7.2) from equation (7.1):

$$\boldsymbol{\omega}_{is}^{s} = \mathbf{R}_{p}^{s}\mathbf{R}_{b}^{p}\mathbf{R}_{m}^{b}\mathbf{R}_{e}^{m}\boldsymbol{\omega}_{ie}^{e} + \mathbf{R}_{p}^{s}\mathbf{R}_{b}^{p}\boldsymbol{\omega}_{mb}^{b} + \boldsymbol{\omega}_{ps}^{s}. \tag{7.2}$$

Here the earth rotation rate can easily be modeled in the e-frame. $\boldsymbol{\omega}_{mb}^{b}$ is known from chapter 3 and $\boldsymbol{\omega}_{ps}^{s}$ can be defined as sensor rotation on the platform. None of the matrices in equation (7.2) depends on the sensors position. Accordingly, a lever arm has not be considered for the simulation of rotation rates. As with accelerometers the gyroscope observation is only in one sensitive axis, so it has to be multiplied from the left side with $(1 \quad 0 \quad 0)$, as well (eq. 7.2). Therefore the scalar observation of the j-th gyroscope $[\omega_{is}^{s}]_{i,j}$ on the platform i reads:

$$[\omega_{is}^{s}]_{i,j} = (1 \quad 0 \quad 0) \cdot \boldsymbol{\omega}_{is}^{s}. \tag{7.3}$$

Additional parameterized sensor errors of the types above can be added and the final simulated observation $\left[l_{gyro}^{s}\right]_{i,j}$ for the gyroscope j on platform i. So the resulting equation is:

$$\left[l_{gyro}^{s}\right]_{i,j} = [\omega_{is}^{s}]_{i,j} \cdot \kappa_{gyro}^{s} + b_{gyro}^{s} + n_{gyro}^{s}. \tag{7.4}$$

8. MAGNETIC FIELD OBSERVATIONS

Another sensor for navigation applications is a magnetic field sensor. It uses the earth magnetic field m_{E}^{e} as a reference frame to orient and to position a body (b) in the e-frame. In the near of the earth surface the field has the shape of a magnetic dipole and points from the magnetic north pole to the magnetic south pole through the earth. The field is thus vertical at the poles and horizontal near the equator. Currently it is inclinated at about 10° to the earth axis of rotation. It shows short-term variations from currents in the ionosphere and magnetosphere and secular variations, which mostly reflect changes in the earth interior. Therefore it is not constant with time. The magnetic field can be described by the magnetic flux density vector m^{n} (x^{e}, t) in the n-frame. It changes its direction and absolute value with position x^{e} and time t. The aberration from geographic north is call declination D, from the horizont inclination I .

A magnetometer observes the magnetic flux density in a single sensitive axis with unit Tesla (T). A model (e.g. World Magnetic Model (WMM) 2010), based on the magnetic potential V, provides the local flux density vector $\mathbf{m}_{mag}^{e}(\mathbf{x}_{mag}^{e}, t)$ on the position of the j-th magnetometer $\mathbf{x}_{mag}^{e}$ at time t in the e-frame as the negative spatial gradient of the scalar potential V. The WMM consists of a spherical-harmonic main field model with order and degree 12 and it is comprised of 168 spherical-harmonic Gauss coefficients. To consider secular variations (SV) of the core field a time-linear model is applied for every Gauss coefficients (Maus et al., 2010).

The input values to the model are the current time and the position of the j-th magnetic field sensor on the i-th platform (p) which is calculated similar to equation (5.1) with eq. (8.1).

$$\left[\mathbf{x}(\mathrm{t})^{\mathrm{e}}_{\mathrm{mag}} = \mathbf{x}(\mathrm{t})^{\mathrm{e}}_{\mathrm{body}} + \mathbf{R}^{\mathrm{e}}_{\mathrm{m}}\mathbf{R}(\mathrm{t})^{\mathrm{m}}_{\mathrm{b}}\mathbf{t}^{\mathrm{b}}_{\mathrm{plat}} + \mathbf{R}^{\mathrm{e}}_{\mathrm{m}}\mathbf{R}(\mathrm{t})^{\mathrm{m}}_{\mathrm{b}}\mathbf{R}^{\mathrm{b}}_{\mathrm{p}}\mathbf{t}^{\mathrm{p}}_{\mathrm{mag}}\right]_{\mathrm{i,j}} \tag{8.1}$$

To model the observations of the magnetometer j on the i-th platform, the magnetic flux density vector $\mathbf{m}^{\mathrm{e}}_{\mathrm{mag}}$ is rotated to the s-frame with equation (8.2).

$$\mathbf{m}^{\mathrm{s}}_{\mathrm{mag}} = \mathbf{R}^{\mathrm{s}}_{\mathrm{p}}\mathbf{R}^{\mathrm{p}}_{\mathrm{b}}\mathbf{R}^{\mathrm{b}}_{\mathrm{m}}\mathbf{R}^{\mathrm{m}}_{\mathrm{e}}\mathbf{m}^{\mathrm{e}}_{\mathrm{mag}}(\mathbf{x}^{\mathrm{e}}_{\mathrm{mag}}, \mathrm{t}) \tag{8.2}$$

Again, by multiplying equation (8.2) with $(1 \quad 0 \quad 0)$ (eq. 8.3), and by considering the sensor error parametrization above in the s-frame, the final observation $\left[\mathrm{l}^{\mathrm{s}}_{\mathrm{mag}}\right]_{\mathrm{i,j}}$ for a magnetometer j is obtained as:

$$\left[\mathrm{m}^{\mathrm{s}}_{\mathrm{mag}}\right]_{\mathrm{i,j}} = (1 \quad 0 \quad 0)\cdot\mathbf{m}^{\mathrm{s}}_{\mathrm{mag}} \quad \text{and} \tag{8.3}$$

$$\left[\mathrm{l}^{\mathrm{s}}_{\mathrm{mag}}\right]_{\mathrm{i,j}} = \left[\mathrm{m}^{\mathrm{s}}_{\mathrm{mag}}\right]_{\mathrm{i,j}} + \mathrm{n}^{\mathrm{s}}_{\mathrm{mag}}. \tag{8.4}$$

9. INCLINOMETER OBSERVATIONS

Another type of sensor especially for orientation giving platforms are inclinometers. An inclinometer j on the platform i measures the declination $[\theta]_{\mathrm{i,j}}$ of the inclinometer axis $\mathbf{s}^{\mathrm{LAV}}_{\mathrm{inc}}$ in respect of the z-axis of the LAV $\mathbf{e}^{\mathrm{LAV}}_{\mathrm{z}}$, defined by the local direction of gravity vector, in the LAV (fig. 3). The inner product (eq. 9.1) of $\mathbf{e}^{\mathrm{LAV}}_{\mathrm{z}}$ and $\mathbf{s}^{\mathrm{LAV}}_{\mathrm{inc}}$ yields the inclination $[\theta]_{\mathrm{i,j}}$:

$$[\theta]_{\mathrm{i,j}} = \cos^{-1}\left(\frac{\mathbf{e}^{\mathrm{LAV}}_{\mathrm{z}}\mathbf{s}^{\mathrm{LAV}}_{\mathrm{inc}}}{|\mathbf{e}^{\mathrm{LAV}}_{\mathrm{z}}||\mathbf{s}^{\mathrm{LAV}}_{\mathrm{inc}}|}\right) \tag{9.1}$$
$$\text{with } \mathbf{e}^{\mathrm{LAV}}_{\mathrm{z}} = (0 \quad 0 \quad 1)^{\mathrm{T}}$$

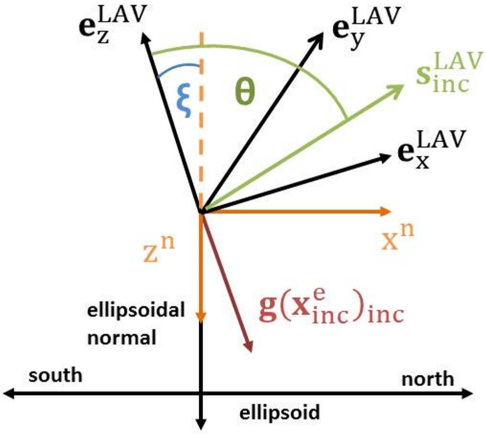
$\mathbf{e}^{\mathrm{LAV}}_{\mathrm{z}}$
$\mathbf{e}^{\mathrm{LAV}}_{\mathrm{y}}$
$\mathbf{s}^{\mathrm{LAV}}_{\mathrm{inc}}$
ξ
θ
$\mathbf{e}^{\mathrm{LAV}}_{\mathrm{x}}$
z^{n}
x^{n}
$\mathbf{g}(\mathbf{x}^{\mathrm{e}}_{\mathrm{inc}})_{\mathrm{inc}}$
ellipsoidal normal
south
north
ellipsoid

Figure 3: Inclinometer observation θ

To obtain the vector $\mathbf{s}^{\mathrm{LAV}}_{\mathrm{inc}}$ the base vector $\mathbf{s}^{\mathrm{s}}_{\mathrm{inc}} = (1 \quad 0 \quad 0)^{\mathrm{T}}$ has to be rotated and it is:

$$\mathbf{s}^{\mathrm{LAV}}_{\mathrm{inc}} = [\mathbf{R}^{\mathrm{LAV}}_{\mathrm{n}}]_{\mathrm{i,j}}\mathbf{R}^{\mathrm{n}}_{\mathrm{b}}\mathbf{R}^{\mathrm{b}}_{\mathrm{p}}\mathbf{R}^{\mathrm{p}}_{\mathrm{s}}\mathbf{s}^{\mathrm{s}}_{\mathrm{inc}}. \tag{9.2}$$

The matrix $[\mathbf{R}^{\mathrm{LAV}}_{\mathrm{n}}]_{\mathrm{i,j}}$ reads:

$$\left[\mathbf{R}^{\mathrm{LAV}}_{\mathrm{n}} = \begin{pmatrix} 1 & -\tan(\mathrm{B})\,\eta & \xi \\ \tan(\mathrm{B})\,\eta & 1 & \eta \\ \xi & \eta & -1 \end{pmatrix}\right]_{\mathrm{i,j}}. \tag{9.3}$$

The matrix $[\mathbf{R}^{\mathrm{LAV}}_{\mathrm{n}}]_{\mathrm{i,j}}$ is dependent on the geographical latitude B of the j-th inclinometer on the i-th platform (p), and the parameters $\xi(\mathrm{B},\mathrm{L},\mathrm{h})$ and $\eta(\mathrm{B},\mathrm{L},\mathrm{h})$, the deflexions of the vertical. Practically due to the moderate extension of bodies and platforms, the body's position is sufficient for modeling (ξ, η). The parameters ξ and η are obtained from a gravity model by standard formulas.

The position of the j-th inclinometer is calculated similar to equation (5.1) with:

$$\left[\mathbf{x}(\mathrm{t})_{\mathrm{inc}}^{\mathrm{e}} = \mathbf{x}(\mathrm{t})_{\mathrm{body}}^{\mathrm{e}} + \mathbf{R}_{\mathrm{m}}^{\mathrm{e}}\mathbf{R}(\mathrm{t})_{\mathrm{b}}^{\mathrm{m}}\mathbf{t}_{\mathrm{plat}}^{\mathrm{b}} + \mathbf{R}_{\mathrm{m}}^{\mathrm{e}}\mathbf{R}(\mathrm{t})_{\mathrm{b}}^{\mathrm{m}}\mathbf{R}_{\mathrm{p}}^{\mathrm{b}}\mathbf{t}_{\mathrm{inc}}^{\mathrm{p}}\right]_{\mathrm{i,j}}. \tag{9.4}$$

The final inclinometer observations result from extention of equation (9.1) together with an additional calibration error c_{inc} and white noise n_{inc} as:

$$[l_{\theta} = \theta + c_{\mathrm{inc}} + n_{\mathrm{inc}}]_{\mathrm{i,j}}. \tag{9.5}$$

10. SIMULATION OF MULTISENSOR ARRAYS (SIMA)

For the validation of new navigation algorithms for GNSS and MEMS-based multi sensor navigation platforms the sensor raw data simulation tool "SIMA" (Simulation of Multisensor Arrays) was developed. SIMA provides individual raw data for a unlimited number of virtual GNSS-sensors ($l_{\mathrm{GNSS-pos}}^{\mathrm{e}}$, $l_{\mathrm{GNSS-vel}}^{\mathrm{e}}$, l_{PR}, l_{ϕ}, $l_{\Delta f}$), accelerometers ($l_{\mathrm{acc}}^{\mathrm{s}}$), gyroscopes ($l_{\mathrm{gyro}}^{\mathrm{s}}$), magnetometers ($l_{\mathrm{mag}}^{\mathrm{s}}$) and/or inclinometers ($l_{\theta}$) to estimate of the state vector $y(t)$. Additionally to the observation data SIMA provides reference data $[\mathbf{l}(\mathrm{t}), \mathbf{y}(\mathrm{t})]_{\mathrm{ref}}$ to verify new implemented algorithms. This includes the standard navigation parameters position $(\mathrm{B}, \mathrm{L}, \mathrm{h})^{\mathrm{e}}$, velocity $(\mathrm{v}_{\mathrm{N}}, \mathrm{v}_{\mathrm{E}}, \mathrm{v}_{\mathrm{D}})^{\mathrm{n}}$ and orientation $(\mathrm{r}, \mathrm{p}, \mathrm{y})_{\mathrm{b}}^{\mathrm{n}}$ in state vector $y(t)$, additional parameter like current rotation rates, accelerations and sensor error parameters. The latter have to be estimated on the fly within the state vector.

The simulation of raw data is performed in three steps at every point of time t. In step one the trajectory of a body (b) is modeled in the m-frame, which is defined by the matrix $\mathrm{R}_{\mathrm{m}}^{\mathrm{e}}(\mathrm{B}_{\mathrm{m-frame}}, \mathrm{L}_{\mathrm{m-frame}})$ depend on the predefined position $\mathrm{x}_{\mathrm{m-frame}}^{\mathrm{e}}$. Based on a predetermined analytic curve and movement characteristics (chapter 3) like a circle, a straight line, a helix or a 2D-trajectory with different route sections the state vector $\mathbf{y}(\mathrm{t})$ is calculated and consists of position $\mathbf{x}(\mathrm{t})_{\mathrm{body}}^{\mathrm{e}}$, velocity $\dot{\mathbf{x}}(\mathrm{t})_{\mathrm{body}}^{\mathrm{e}}$, acceleration $\ddot{\mathbf{x}}(\mathrm{t})_{\mathrm{body}}^{\mathrm{e}}$, orientation $\mathbf{R}(\mathrm{t})_{\mathrm{b}}^{\mathrm{m}}$, rotation rate $\mathbf{\Omega}(\mathrm{t})_{\mathrm{mb}}^{\mathrm{b}}$ and rotation rate change $\dot{\mathbf{\Omega}}(\mathrm{t})_{\mathrm{mb}}^{\mathrm{b}}$ of the body (b) in the e- or rather the b-frame.

In the second step sensor raw data are calculated accordingly chapters (5-9) either for an over-determined or optionally for a standard sensor configuration (1 GNSS, 1 IMU triad). According to the lever arm concept described in chapter (4), virtual platforms (p) can be positioned and orientated individually on the body (b) with lever arm parameters $\left[\mathbf{t}_{\mathrm{plat}}^{\mathrm{b}}, \mathbf{R}_{\mathrm{p}}^{\mathrm{b}}(\mathrm{r}, \mathrm{p}, \mathrm{y})\right]_{\mathrm{i}}$. On each platform (p) any number of sensors can be positioned and orientated with the parameters $\left[\mathbf{t}_{\mathrm{sensor}}^{\mathrm{p}}, \mathbf{R}(\alpha, \delta)_{\mathrm{s}}^{\mathrm{p}}\right]_{\mathrm{i,j}}$.

In step three individual sensor error parametrizations like bias, scale factor or specific sensor noise can be added to every sensor j on the i-th platform (p) that leads to sensor specific observations. Additional occasional gross sensor errors can also be simulated in SIMA.

All in all, SIMA allows the development of loose and tight coupled navigations algorithms based on simulated raw data with a known reference trajectory $[\mathbf{l}(\mathrm{t}), \mathbf{y}(\mathrm{t})]_{\mathrm{ref}}$ under consideration of the lever arm effects in every sensor j without any constraints to the geomatrical design and the number of sensors.

The stepwise software concept allows an integration of more sophisticated error models dependent on time, driving forces and temperature for GNSS, inclinometers or MEMS-sensors. Additional sensor observations e.g. barometers can be implemented and the SIMA can be extended with new trajectories.

11. EXAMPLES

11.1 3D-ORIENTATION-FILTER

To validate the implementation of SIMA an error state Kalman filter from literature was choosen (Farrell, 2008) to calculate a navigation solution with SIMA's raw data and compare the result with SIMA's reference data. This filter is an attitude and heading reference system (AHRS) to estimate the orientation R_b^n of a body (b) in respect to the n-frame. This approach integrates the observations from a gyroscope triad through the attitude kinematics equations and is aided with an accelerometer and a magnetometer sensor triad. Additionally to the attitude quaternion q_b^n, the biases of the gyroscopes $\boldsymbol{b}_{gyro}^s$ and accelerometers $\boldsymbol{b}_{acc}^s$ are estimated in the filter state $\mathbf{y}(\mathrm{t})$ (4).

$$\mathbf{y}(\mathrm{t}) = \left[\mathbf{q}_{\boldsymbol{b}}^{\boldsymbol{n}}, \mathbf{b}_{\mathrm{gyro}}^{s}, \mathbf{b}_{\mathrm{acc}}^{s}\right]^{\mathrm{T}} \tag{11.1}$$

The observations are simulated for a body (b), which is in rest at B=0 und L=0 with $\boldsymbol{R}_m^e(0{,}0)$ and rotates with rotation rates of $\omega_{\mathrm{mb,x}}^{\mathrm{b}} = 10\ °/s$, $\omega_{\mathrm{mb,y}}^{\mathrm{b}} = 20\ °/s$ and $\omega_{\mathrm{mb,z}}^{\mathrm{b}} = 30\ °/s$. In figure (4) the raw accelerometer observations with biases $\boldsymbol{b}_{acc}^s = (1.0 \quad 2.0 \quad 3.0)$ m/s^2 are presented. The result can be seen in figure (5). At the beginning the filtered pitch angle p_b^n of the body differs strongly from the reference angle because of the large bias errors in the accelerometers and gyroscopes. After about eight seconds their biases are almost estimated correctly (fig. 6). That results in a very close estimation of the orientation in regard to the reference.

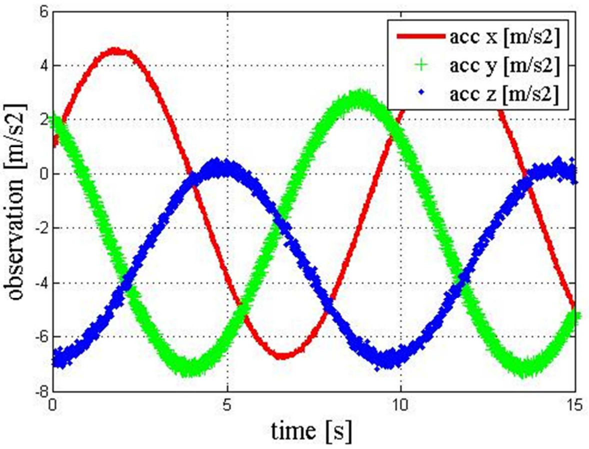

Figure 4: Raw data observations of accelerometers

11.2 2D-BOAT-FILTER

For the navigation of a boat a restrictive algorithm related to the horizontal position and orientation was developed in the scope of the Baden-Württemberg joint RaD *project "GNSS/INS and multi-sensor navigation algorithms and platforms for mobile navigation and object geo-referencing"*(www.navka). The state vector $\mathrm{y(t)}$ (eq. 11.4) consists of the body position $(\mathrm{B,L})^{\mathrm{e}}$, absolute velocity v and acceleration a, the yaw angle $\mathrm{y_b^n}$ in respect to the n-

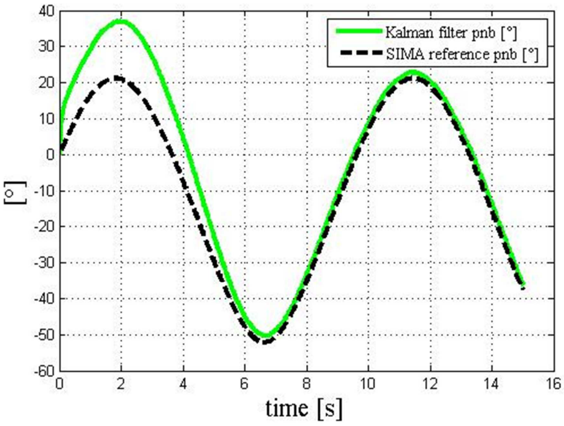

Figure 5: Kalman filter result of pitch angle p_b^n and SIMA reference data

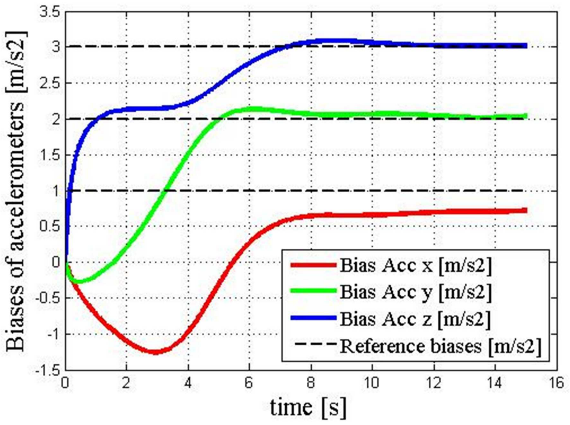

Figure 6: Estimated accelerometer biases und true bias from SIMA

frame, the rotation rate $\omega_{ib,z}^{b}$ of the body z-axis in respect to the i-frame in the b-frame and a bias $b_{gyro}^{s}$for the gyroscope and reads:

$$\mathbf{y}(t) = \left[(B,L)^e|(v,a)|y_b^n\middle|\omega_{ib,z}^b\middle|b_{gyro}^s\right]^T. \tag{11.4}$$

To showcase the lever arm effects on a GNSS receiver two GNSS-receivers and a gyroscope are simulated to observe the state $y(t)$. The first GNSS receiver is placed in the body origin, whereas the second receiver has a lever arm of 20 meters in x-axis of the body frame with $t_{sensor}^{p} = [20 \quad 0 \quad 0]^T$, the offset parameter of the gyroscope is assumed to be 28.7°/sec. Both GNSS-position observations are presented in figure (7). It can be noticed, that the second GNSS receiver has a systematic offset, which is correct and caused by the lever arm in x. Because this lever arm is considered in the filter observation equation, too, the filtered position of the body is on the correct reference trajectory. In figure (8) the bias error estimation of the gyroscope is presented. The simulated error of 28.7° is reached after 20s.

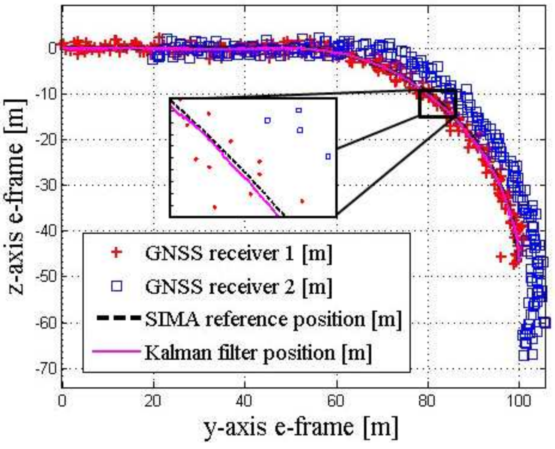

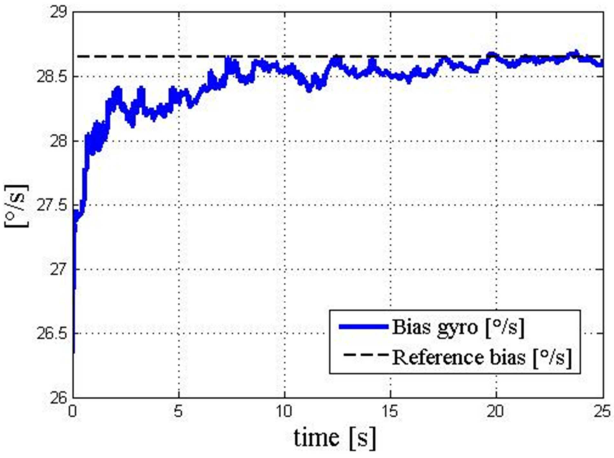

Figure 7: GNSS positions with lever arm of 20m, reference trajectory and filter results

Figure 8: Filtered estimation of gyroscope bias in comparison to reference value

12. ACKNOWLEDGEMENT

The funding of the Joint Research Project „GNSS/INS and multi-sensor navigation algorithms and platforms for mobile navigation and object geo-referencing“ for three years (2011-2013) by the Ministry of Economics and the navigation and mobile IT industry of Baden-Württemberg is gratefully acknowledged. The objective of the research team 'NAVKA' at the central research center at the Institute of Applied Research (IAF) at University of Applied Sciences Karlsruhe is to develop robust algorithms for multi-sensor GNSS and MEMS-based platforms (p) for the navigation of arbitrary bodies (b) and for mobile indoor and outdoor geo-referencing applications independent from extern infrastructure.

REFERENCES

[1] Farrell J. (2008): *Aided Navigation: GPS with High Rate Sensors*, Mc Graw Hill

[2] Hofmann-Wellenhof B., Lichtenegger H., Collins J. (1992): *GPS – Theory and Practice*, 3.rd edition, Springer Verlag New York

[3] Jekeli C. (2001): *Inertial Navigation Systems with Geodetic Applications*, Walter de Gruyter, Berlin

[4] Kaplan E., Hegarty C. (2006): *Understanding GPS – Principles and Applications*, 2nd edition, Artech House, London

[5] Maus S., S. Macmillan, S. McLean, B. Hamilton, A. Thomson, M. Nair, and C. Rollins, (2010): *The US/UK World Magnetic Model for 2010-2015*, NOAA Technical Report NESDIS/NGDC

[6] Seeber G. (2003): *Satellite Geodesy*, 2nd edition, Walter de Gruyter, Berlin

[7] Torge W. (2003): *Geodäsie*, Walter de Gruyter, Berlin

[8] Wendel J. (2007): *Integrierte Navigationssysteme*, Oldenbourg Verlag, München

BIOGRAPHICAL NOTES

Prof. Dr.-Ing. Reiner Jäger
Professor for Satellite and Mathematical Geodesy, Adjustment and Software Development at Karlsruhe University of Applied Sciences (HSKA)
Head of the Laboratory of GNSS and Navigation, of the Institute of Geomatics at IAF and of the joint RaD project "GNSS-supported lowcost multisensor systems for mobile platform navigation and object geo-referencing" (www.navka.de)
Member FIG Commission 5 WG 5.4 Kinematic Measurements

CONTACTS

Prof. Dr.-Ing. Reiner Jäger
University of Applied Sciences – Institute of Applied Research (IAF)
Moltkestraße 30
76137 Karlsruhe
GERMANY
Tel. +49 (0)721 925-2620
Fax +49 (0)721 925-2591
Email: Reiner.Jaeger@HS-Karlsruhe.de
Web site: www.navka.de